12^{th} International Conference on Fracture Mechanics of Concrete and Concrete Structures
FraMCoS-12
B.L.A. Pichler, Ch. Hellmich, P. Preinstorfer (Eds)

https://doi.org/10.21012/FC12.1305
MS18-1:3

COMPARISON OF CONVENTIONAL AND LOCALIZING GRADIENT ENHANCEMENTS FOR CONCRETE DAMAGE-PLASTICITY MODELS

A. DUMMER*, M. NEUNER† AND G. HOFSTETTER*

* University of Innsbruck, Institute of Basic Sciences in Engineering Sciences, Innsbruck, Austria
e-mail: alexander.dummer@uibk.ac.at, guenter.hofstetter@uibk.ac.at

†University of Natural Resources and Life Sciences, Institute of Structural Engineering, Vienna, Austria
e-mail: matthias.neuner@boku.ac.at

Key words: Quasi-Brittle Failure, Gradient-Enhanced Continuum, Plasticity, Damage Mechanics

Abstract. Cracking in quasi-brittle materials, like concrete, is known to be a nonlocal process associated with an intrinsic material length scale. To take into account these nonlocal effects in continuum damage models for concrete, many approaches have been proposed in the past decades. The latter comprise integral nonlocal formulations, implicit or explicit gradient-enhanced models, as well as the phase field approach to cohesive fracture. Among them, implicit gradient-enhanced models have proved to represent a powerful approach, when applied in Finite Element simulations. However, it is well-known that conventional gradient-enhanced models yield a nonphysical broadening of the damaged zone. To overcome this issue, the so-called localizing gradient damage model with decreasing interaction has been proposed by Poh and Sun. However, to the authors' best knowledge, this formulation has only rarely been applied to damage-plasticity models, and a comprehensive discussion of its impact on the structural behavior is missing in the literature. In this study, we investigate the localizing gradient formulation proposed by Poh and Sun for the widely recognized concrete damage-plasticity (CDP) model by Grassl and Jirásek. Specifically, we discuss the advantages and disadvantages compared to the conventional gradient enhancement through a simple 1D tensile test and a numerical benchmark example.

1 Introduction

The appropriate and accurate modeling of concrete failure has been the topic for many research groups in the past decades. Developed models can be divided into discrete approaches, in which the separation of material is taken into account, and continuum approaches, where cracks are described in an approximative smeared manner. For the latter, in the course of modeling material softening, regularization techniques are key ingredients for meaningful, i.e., discretization insensitive, results in numerical simulations. From a material characterization point of view these discretization-sensitive results originate from not taking material-specific length parameters into account, when using unregularized classical continuum models.

So-called generalized continuum models, which naturally take internal length parameters into account, provide a remedy for this issue. The class of generalized continuum models comprises, e.g., (i) explicit or implicit gradient-enhanced models [8], (ii) integral nonlocal formulations [1, 4], (iii) micropolar or Cosserat type models [6], and (iv) the phase-field approach to fracture [5] Among them, models based on the continuum

enhanced with gradients of internal variables have gained widespread acceptance for modeling quasi-brittle failure of concrete, cf. e.g., [7, 13, 6, 2]. In the most simple version, the length of nonlocal interaction is assumed to be constant, termed as the *conventional* approach in the following. This results in a nonphysical broadening of the damaged zone which is not in accordance with experimental observations. To overcome this issue, the so-called gradient damage model with decreasing interactions has been proposed by Poh and Sun [9]. This approach is termed as the *localizing* approach in the following. Thereby, the nonlocal interaction decreases with growing damage, preventing the spurious growth of the damaged zone. Since the introduction of the localizing gradient damage model, this technique has been mostly applied to damage models for concrete. To the author's best knowledge, only Zhao et al. [12] applied the localizing gradient enhancement to a damage-plasticity model for concrete. The authors confirmed to overcome the issues of the spurious growth of the damaged zone, and to obtain mesh-insensitive results in numerical simulations. However, a rigorous and critical discussion on the applicability and limitations of the approach is missing in the respective publication. This is the motivation of the present contribution. We investigate the straightforward extension of a well-established damage-plasticity model for concrete, firstly using a simple 1D tensile test, and subsequently using a well-known benchmark example for concrete failure.

The remainder of this contribution is organized as follows: In Section 2, we briefly summarize the general structure of the gradient-enhanced damage-plasticity models. Subsequently, we discuss the differences between conventional and localizing gradient-enhancements by means of a simple 1D tensile test in Section 3. In Section 4, we briefly introduce the concrete damage-plasticity model by Grassl and Jirásek [3], and compare both, conventional and localizing gradient enhancements, using a well-known benchmark example for concrete failure. Based on the presented results, Section 5 provides a summary, discussion, and an outlook on important future research directions.

2 Gradient-enhanced damage-plasticity models for concrete

In the gradient-enhanced continuum theory [8], the quasi-static equilibrium equation

$$\nabla \boldsymbol{\sigma} + \boldsymbol{f} = \boldsymbol{0}, \tag{1}$$

in which $\boldsymbol{\sigma}$ is the Cauchy stress tensor and $\boldsymbol{f}$ denotes the body forces, forms a coupled system of partial differential equations, together with the second-order partial differential equation

$$\bar{\beta} - c\,\Delta\bar{\beta} = \alpha_{\mathrm{d}}, \tag{2}$$

which describes the integrity of the material. In Eq. (2), $\bar{\beta}$ denotes the nonlocal damage driving variable, and α_{d} is its local counterpart. The parameter c controls the length of nonlocal interaction which may change during the loading process. Poh and Sun [9] employ a slightly different second-order partial differential equation for the nonlocal variable:

$$\bar{\beta} - \nabla(c\nabla\bar{\beta}) = \alpha_{\mathrm{d}}. \tag{3}$$

Note that the latter equation is equivalent to Eq. (2) only for constant c. In this contribution, we adopt Eq. (3) for describing the nonlocal variable.

For a coupled damage-plasticity approach with isotropic damage, the stress-strain relation is expressed in rate form as

$$\dot{\boldsymbol{\sigma}} = (1-\omega)\,\mathbb{C} : (\dot{\boldsymbol{\varepsilon}} - \dot{\boldsymbol{\varepsilon}}^{\mathrm{p}}) - \dot{\omega}\,\mathbb{C} : (\boldsymbol{\varepsilon} - \boldsymbol{\varepsilon}^{\mathrm{p}}), \tag{4}$$

in which $\mathbb{C}$ denotes the fourth-order elastic stiffness tensor, and $\boldsymbol{\varepsilon}$ and $\boldsymbol{\varepsilon}^{\mathrm{p}}$ are the total strain tensor and the plastic strain tensor, respectively. Furthermore, ω denotes the isotropic damage variable which is computed from the nonlocal damage driving variable $\bar{\beta}$.

The elastic domain is delimited by the yield function $f_{\mathrm{p}}(\bar{\boldsymbol{\sigma}}, q_{\mathrm{h}})$, formulated in terms of the effective stress tensor $\bar{\boldsymbol{\sigma}} = \boldsymbol{\sigma}/(1-\omega)$, and an internal hardening variable q_{h}.

The evolution of the plastic strain $\boldsymbol{\varepsilon}^{\mathrm{p}}$ may then be described utilizing a non-associated flow rule as

$$\dot{\boldsymbol{\varepsilon}}^{\mathrm{p}} = \dot{\lambda}\,\frac{\partial g_{\mathrm{p}}(\bar{\boldsymbol{\sigma}})}{\partial \bar{\boldsymbol{\sigma}}}, \tag{5}$$

with the plastic multiplier $\dot{\lambda}$ and the plastic potential function g_{p}.

3 Simple 1D tensile test

To start a detailed analysis of conventional and localizing gradient-enhanced damage-plasticity models, we consider a simple 1D tensile test, cf. Fig. 1. The specimen is assumed to be of length $2L$ with the constant cross-sectional area A. For triggering the damage process, a slightly weakened zone of length $2\kappa L$ is assumed in the center of the specimen.

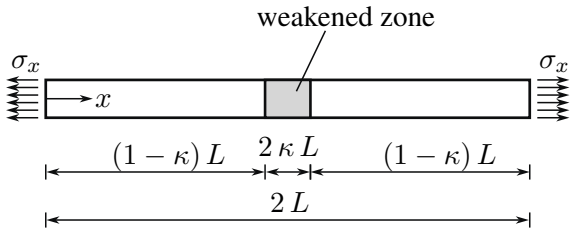

Figure 1: Simple 1D tensile test with a weakened zone in the center.

The material behavior is assumed as linear elastic, perfectly plastic, and softening in the post-peak regime. The following constitutive equations represent the 1D tensile behavior predicted by the concrete damage-plasticity model by Grassl and Jirásek [3] which will be used in the Finite Element simulations later on. The equations for 1D tensile loading are given as follows. The stress-strain relation reads

$$\sigma_x = (1-\omega)\,E\,(\varepsilon_x - \varepsilon_x^{\mathrm{p}}), \tag{6}$$

where σ_x is the axial stress, E is the Young's modulus, and ε_x and $\varepsilon_x^{\mathrm{p}}$ denote the total and plastic axial strain, respectively. The elastic domain is delimited by the yield function

$$f_{\mathrm{p}}(\bar{\sigma}_x) = |\bar{\sigma}_x| - f_{\mathrm{tu}} \tag{7}$$

in which $\bar{\sigma}_x$ is the effective axial stress, and f_{tu} is the uniaxial tensile strength. The evolution of the plastic strain is described by the associated flow rule

$$\dot{\varepsilon}_x^{\mathrm{p}} = \dot{\lambda}\frac{\partial f_{\mathrm{p}}}{\partial \bar{\sigma}_x} = \dot{\lambda}\frac{\sigma_x}{|\sigma_x|}, \tag{8}$$

with the plastic multiplier $\dot{\lambda}$. For describing the evolution of damage the exponential softening law

$$\omega = 1 - \exp(-\bar{\beta}/\epsilon_{\mathrm{f}}) \tag{9}$$

is employed. Therein, ϵ_{f} controls the steepness of the softening curve. The nonlocal damage driving variable is computed from the 1D version of equation (3)

$$\bar{\beta} - (c\,\bar{\beta}')' = \alpha_{\mathrm{d}}, \tag{10}$$

where $(\bullet)'$ denotes the first-order spatial derivative with respect to the coordinate x. The evolution of the local damage driving force is defined as

$$\dot{\alpha}_{\mathrm{d}} = |\dot{\varepsilon}_x^{\mathrm{p}}| = \dot{\lambda}. \tag{11}$$

Conventional approach. In the case of a conventional gradient-enhanced formulation, i.e., $c = c_0$ (constant), Eq. (10) can be solved analytically for the simple tensile test shown in Fig. 1. In the following, the symmetry of the problem is exploited, and only the solution for the left half of the specimen, i.e., $0 \leq x \leq L$, is considered. This is achieved by assuming an incremental increase of the plastic strain in the weakened zone, resulting in the same incremental increase of the local damage driving force. Plastic deformations are only present in the weakened zone, and thus, the solution is split into two regions. The solution for the nonlocal damage driving field of the unweakened zone, i.e., $x < \kappa L$, is given by the homogeneous solution of Eq. (10)

$$\bar{\beta}_1(x) = A_1 \exp\left(x/\sqrt{c_0}\right) + B_1 \exp\left(-x/\sqrt{c_0}\right), \tag{12}$$

where A_1 and B_1 are integration constants. The solution for the nonlocal damage driving field of the weakened zone, i.e., $\kappa L \leq x \leq L$,

is given by the solution of the inhomogeneous Eq. (10)

$$\bar{\beta}_2(x) = A_2 \exp(x/\sqrt{c_0}) + B_2 \exp(-x/\sqrt{c_0}) + C, \tag{13}$$

where A_2 and B_2 are integration constants, and the constant C refers to the particular solution.

The constants A_1, B_1, A_2 and B_2 are determined by the Neumann boundary condition, i.e., $\bar{\beta}'(0) = 0$, the symmetry condition, i.e., $\bar{\beta}'(L) = 0$, as well as the continuity requirements, i.e., $\bar{\beta}_1(\kappa L) = \bar{\beta}_2(\kappa L)$ and $\bar{\beta}_1'(\kappa L) = \bar{\beta}_2'(\kappa L)$.

With the known nonlocal damage driving field, the damage variable ω can be computed from the softening law (9). The equilibrium equation (1) requires constant stress along the specimen, which is the elastic solution in the pre-peak regime. The stress in the post-peak regime is determined at the cross-section with the maximum damage, i.e., at $x = L$ due to symmetry. Thus, the stress along the specimen is constant and is computed as

$$\sigma_x = (1 - \omega_{\max}) f_{\text{tu}}, \tag{14}$$

Next, the strain distribution along the specimen can be computed as

$$\varepsilon_x = \frac{\sigma_x}{(1-\omega)E} + \varepsilon_x^{\text{p}} \tag{15}$$

with the known plastic strain distribution which is constant in the weakened zone, and zero elsewhere.

Localizing approach. Following the localizing gradient-enhanced approach by Poh and Sun [9], the nonlocal interaction parameter is assumed to decrease with growing damage. This results in a nonlocal interaction parameter as a function of the damage variable, i.e., $c(\omega) = g(\omega)\, c_0$, with the scaling function

$$g(\omega) = \frac{(1-R)\exp(-\eta\,\omega) + R - \exp(-\eta)}{1 - \exp(-\eta)} \tag{16}$$

in which R is a parameter controlling the minimum interaction, and η is a parameter controlling the steepness of the decrease. In this contribution, we use the default values $R = 0.005$ and $\eta = 5$ as proposed in [9].

Because the nonlocal interaction parameter is now a function of the damage variable, and thus a function of the nonlocal damage driving field, the governing equation for the nonlocal field (10) becomes a *nonlinear* ordinary differential equation. Consequently, an analytical solution is hard, if not impossible, to find. Thus, for computing the nonlocal damage driving field, the Finite Difference Method (FDM), together with an iterative Newton-Raphson scheme is employed. Once the nonlocal damage driving field is known, the procedure for computing the damage variable ω, stress, and strain distribution is the same as for the conventional gradient-enhanced model.

Parameters and results. The parameters for the 1D tensile test are given in Table 1. The strength and stiffness parameters are chosen in line with the experiments on L-shaped specimens by Winkler et al. [11], as the respective experiments are simulated in the next section. The softening modulus ϵ_{f} is calibrated for the fixed interaction parameter c_0 such that the experimentally determined mode I fracture energy of $G_{\text{f}}^{(\text{I})} = 74\,\text{J/m}^2$ is obtained in the tensile test. This results in different values of ϵ_{f} for the conventional and localizing gradient-enhanced model.

Table 1: Parameters for the 1D tensile test.

Parameter	Value
Young's modulus E	25.8 GPa
Uniaxial tensile strength f_u	2.7 MPa
Softening modulus ϵ_{f}	
conventional	4.64×10^{-4}
localizing	1.35×10^{-3}
Nonlocal length parameter $\sqrt{c_0}$	25 mm
Specimen length $2L$	0.2 m
Weakened zone parameter κ	0.05

Fig. 2 shows the distribution of α_d, $\bar{\beta}$, ω, and the total strain ε_x along the specimen length for the 1D tensile test at different values of the plastic strain in the weakened zone. It can be seen, that the damage variable ω is distributed along the whole specimen length, and the damaged zone is broadened due to the constant nonlocal interaction parameter. The widespread damage is also reflected in the strain distribution.

Fig. 3 shows the distribution of the same variables along the specimen for the localizing gradient-enhanced model. It can be seen that the damaged zone does not broaden during the loading process, which is attributed to the decreasing nonlocal interaction parameter. Furthermore, the strain distribution is more localized in the middle of the specimen.

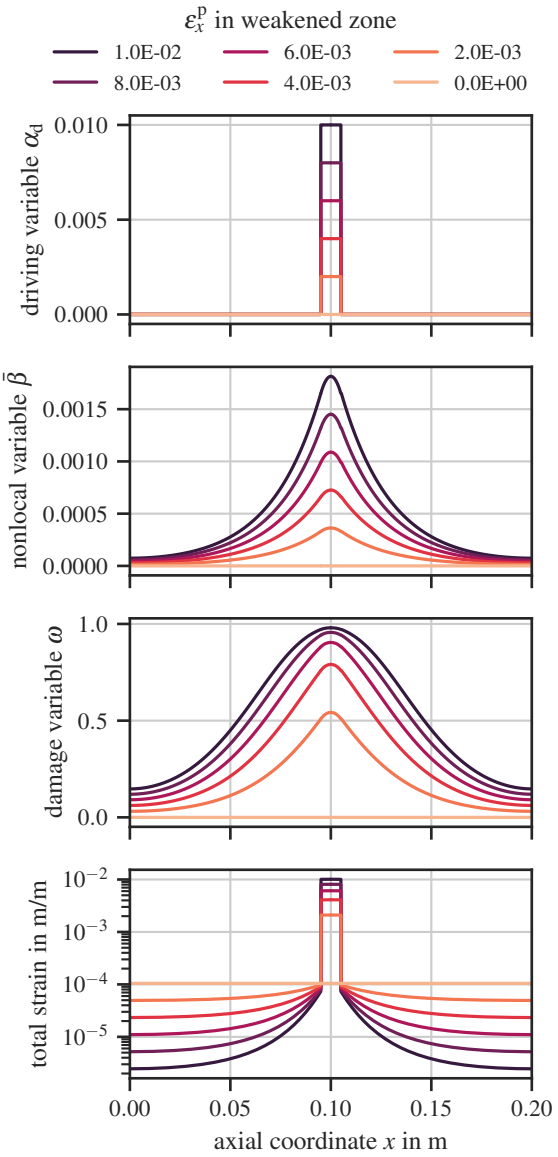

Figure 2: Distribution of different variables along the specimen length for the conventional gradient-enhanced model: local driving variable α_d (top), nonlocal variable $\bar{\beta}$, damage variable ω, and total strain (bottom) for increasing plastic strain values in the weakened zone.

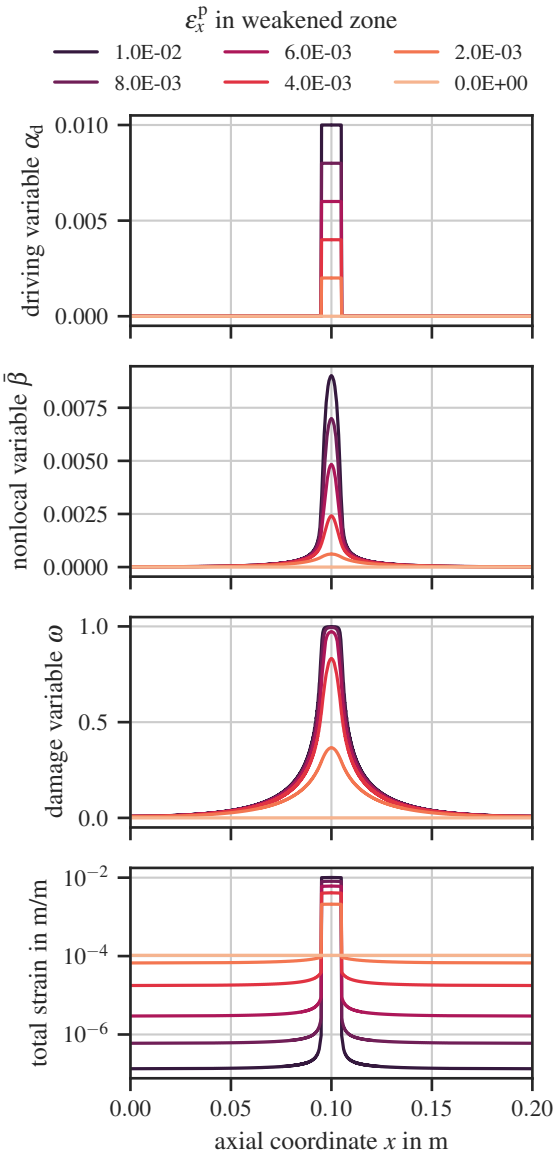

Figure 3: Distribution of different variables along the specimen length for the localizing gradient-enhanced model: local damage driving variable α_d (top), nonlocal variable $\bar{\beta}$, damage variable ω, and total strain (bottom) for increasing plastic strain values in the weakened zone.

The load-displacement curves for both, the conventional and localizing gradient-enhanced model are shown in Fig. 4. Significant differences are observed in the post-peak regime. For the conventional approach, the exponential softening law can directly be identified, whereas a S-shaped deviation from the exponential softening law is obtained for the localizing gradient-enhanced model.

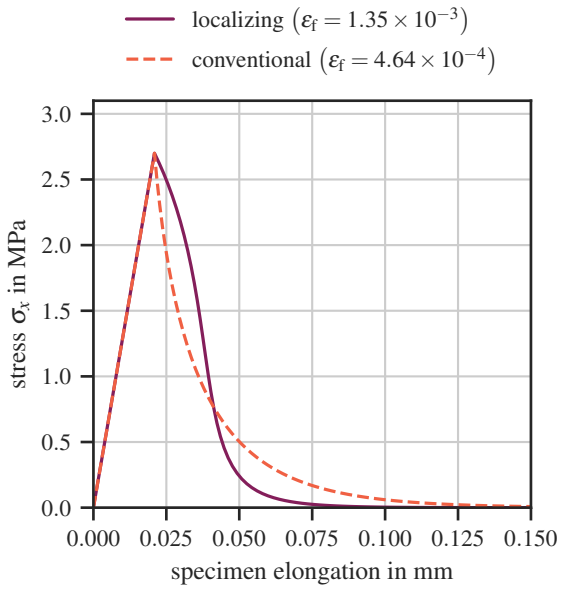

Figure 4: Load-displacement curve for the 1D tensile test: conventional vs. localizing gradient-enhanced model.

In summary, both approaches have advantages and disadvantages. In particular, for the conventional approach, the undesired broadening of the damaged zone is observed, However, the load-displacement curve, shows the expected exponential slope of the softening law. By contrast, the damage pattern and strain distribution resulting from the localizing approach are more realistic, i.e., the damaged zone does not broaden during the loading process. However, the load-displacement curve has a S-shaped form, which is not expected for direct tensile tests of concrete specimens.

So far, only the behavior under 1D tension has been studied, which does not allow any conclusions to be drawn on the structural behavior in 3D Finite Element simulations.

4 Finite Element simulations

In the upcoming section, we briefly review the concrete damage-plasticity model proposed by Grassl and Jirásek [3]. Both, conventional and localizing gradient enhancements, are compared and discussed in the context of numerical simulations of the well-known tests on L-shaped specimens carried out by Winkler et al. [11].

Test setup. The test setup used by Winkler et al. [11] is illustrated in Fig. 5. The specimen was loaded in the vertical direction by a prescribed displacement. Simultaneously, the load-displacement curve was recorded. In the numerical simulations, the shaded regions are modeled as linear elastic, because of the reinforcement. The remaining part of the specimen is modeled using the concrete damage-plasticity model.

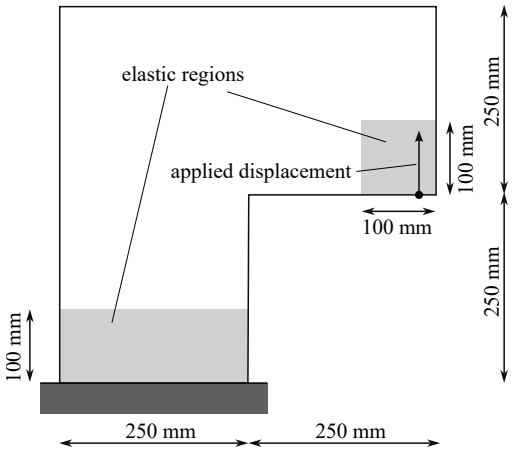

Figure 5: Test setup for the L-shaped specimen test by Winkler et al. [11].

Constitutive model. To describe the nonlinear material behavior of concrete, the concrete damage-plasticity model by Grassl and Jirásek [3] is employed. Thereby, the elastic domain is delimited by the yield function

$$f_{\mathrm{p}}(\bar{\boldsymbol{\sigma}}, q_{\mathrm{h}}(\alpha_{\mathrm{p}})) = \left((1 - q_{\mathrm{h}}(\alpha_{\mathrm{p}})) \left(\frac{\bar{\rho}}{\sqrt{6} f_{\mathrm{cu}}} + \frac{\bar{\sigma}_{\mathrm{m}}}{f_{\mathrm{cu}}} \right)^2 + \sqrt{\frac{3}{2}} \frac{\bar{\rho}}{f_{\mathrm{cu}}} \right)^2 + m_0 \, q_{\mathrm{h}}^2(\alpha_{\mathrm{p}}) \left(\frac{\bar{\rho}}{\sqrt{6} f_{\mathrm{cu}}} r(\theta) + \frac{\bar{\sigma}_{\mathrm{m}}}{f_{\mathrm{cu}}} \right) - q_{\mathrm{h}}^2(\alpha_{\mathrm{p}}), \tag{17}$$

formulated in terms of three invariants of the effective stress tensor, i.e., the effective mean stress $\bar{\sigma}_{\mathrm{m}}$, the effective deviatoric radius $\bar{\rho}$ and the LODE angle θ, as In Eq. (17), $r(\theta)$ is a function proposed by Willam and Warnke [10] defining the shape of the yield function in the deviatoric sections, q_{h} denotes the normalized stress-like internal hardening variable, and m_0 is the friction parameter, defined in terms of the material strength parameters, i.e., the uniaxial compressive strength $f_{\mathrm{cu}}(t)$, the uniaxial tensile strength $f_{\mathrm{tu}}(t)$ and the equi-biaxial compressive strength $f_{\mathrm{cb}}(t)$. The evolution of the plastic strain $\boldsymbol{\varepsilon}^{\mathrm{p}}$ is described using a non-associated flow rule, cf. Eq. (5), using the plastic potential function

$$g_{\mathrm{p}}(\bar{\sigma}_{\mathrm{m}}, \bar{\rho}, q_{\mathrm{h}}(\alpha_{\mathrm{p}})) = \left((1 - q_{\mathrm{h}}(\alpha_{\mathrm{p}})) \left(\frac{\bar{\rho}}{\sqrt{6} f_{\mathrm{cu}}} + \frac{\bar{\sigma}_{\mathrm{m}}}{f_{\mathrm{cu}}} \right)^2 + \sqrt{\frac{3}{2}} \frac{\bar{\rho}}{f_{\mathrm{cu}}} \right)^2 + q_{\mathrm{h}}^2(\alpha_{\mathrm{p}}) \left(\frac{m_0 \, \bar{\rho}}{\sqrt{6} f_{\mathrm{cu}}} + \frac{m_{\mathrm{g}}(\bar{\sigma}_{\mathrm{m}})}{f_{\mathrm{cu}}} \right). \tag{18}$$

where m_0 and $m_{\mathrm{g}}(\bar{\sigma}_{\mathrm{m}})$ are parameters controlling the plastic dilation.

The evolution of the isotropic damage variable ω is governed by the exponential softening law Eq. (9). For computing the local damage driving force α_{d} in Eq. (2), the equivalent plastic strain rate is defined according to [3] as

$$\dot{\alpha}_{\mathrm{d}}^{(\mathrm{p})} = \begin{cases} 0 & \text{if } \alpha_{\mathrm{p}} < 1, \\ \dot{\varepsilon}_{\mathrm{V}}^{\mathrm{p}} / x_{\mathrm{s}}(\dot{\boldsymbol{\varepsilon}}^{\mathrm{p}}) & \text{otherwise,} \end{cases} \tag{19}$$

in which $\dot{\varepsilon}_{\mathrm{V}}^{\mathrm{p}}$ denotes the volumetric part of the plastic strain rate, and $x_{\mathrm{s}}(\dot{\boldsymbol{\varepsilon}}^{\mathrm{p}})$ is a function controlling the post-peak ductility. The parameter α_{p} is an internal strain hardening variable, for which $\alpha_{\mathrm{p}} = 1$ represents the fully hardened state, i.e., indicating that the material strength is reached. For uniaxial tension $x_s = 1$, thus the simple 1D model used in the previous section is the specialization of the present model for 1D tension.

Numerical model. The L-shaped domain is discretized with 20 node hexahedral elements with quadratic shape functions using three different mesh sizes. The mesh sizes coarse (25 mm), medium (8.3 mm), and fine (2.8 mm) refer to approximate element sizes in the area of the expected crack. The material parameters are chosen according to the standard tests conducted in the course of the experiments by Winkler et al. [11]. The same key parameters are chosen as for the 1D tensile test, which are summarized in Table 1. Since no calibration of the material parameters is performed in this contribution, the following results can be interpreted as a blind prediction.

Numerical results. Fig. 6 shows a typical damage contour on the fine mesh in the post peak regime for both, the conventional and localizing approaches. The damaged zone is nonphysically wide for the conventional approach, while the localizing approach yields a more localized damage zone. So far, the localizing approach seems to outperform the conventional approach. However, the nonlocal interaction parameter is chosen relatively large, and a more localized damage pattern could be observed with a smaller parameter using the conventional approach, see e.g., Neuner et al. [6]. Nevertheless, also a smaller nonlocal interaction parameter leads to a broadening of the damaged zone during the loading process.

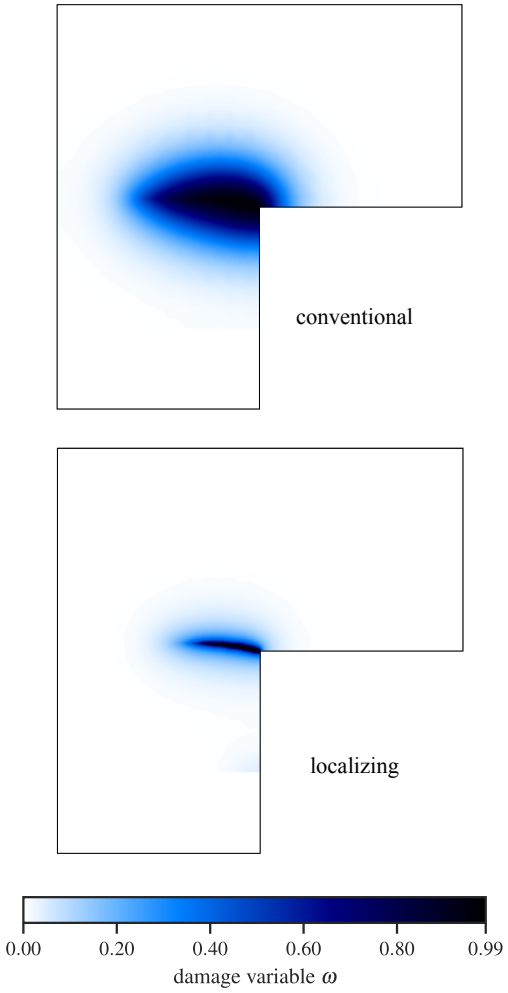

Figure 6: Typical contour plot of the damage variable ω using the fine mesh for the conventional approach (top) and the localizing approach (bottom).

Fig. 7 shows the load-displacement curves for the L-shaped specimen obtained in the FE simulations with three different mesh sizes, together with the experimental data observed by by Winkler et al. [11]. It can be seen that the conventional gradient-enhanced model yields a good prediction of the ultimate load, and the results for the medium and fine mesh are almost identical. By contrast, the localizing gradient-enhanced model overestimates the ultimate load significantly. Additionally, the simulations for the fine and medium mesh terminated early, which may be due to instabilities and oscillations arising in the nonlocal damage driving field. Moreover, the results between the medium and fine mesh differ considerably. This confirms that the localizing gradient-enhanced model needs a by far more refined mesh to obtain meaningful results. This is of course not surprising, as the nonlocal interaction parameter decreases with growing damage, and thus the nonlocal interactions are more localized, and can thus only be resolved with a very fine mesh.

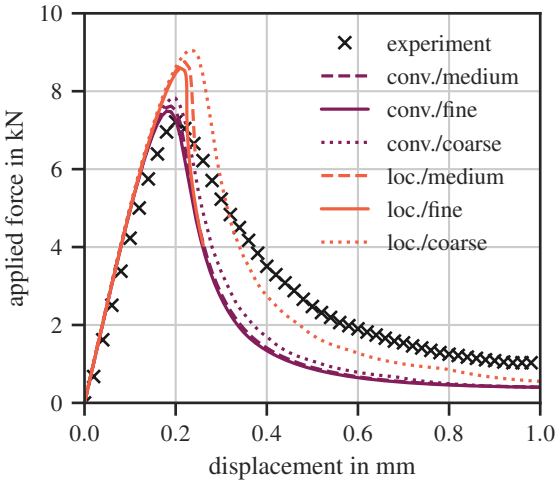

Figure 7: Load-displacement curves for the L-shaped specimen test by Winkler et al. [11].

5 Conclusions and outlook

In this contribution, we compared conventional and localizing gradient-enhancements for a specific, well-established concrete damage-plasticity model. The comparison includes a simple 1D tensile test and numerical simulations of the L-shaped specimen test by Winkler et al. [11]. The following conclusions can be drawn:

- As already known from previous studies, the conventional gradient-enhanced model yields a broadened damage zone in both simple 1D tensile tests and structural simulations. However, the prediction of the structural behavior, i.e., the maximum load carrying capacity, in the L-shaped specimen test is appropriate.
- The naive straight-forward extension of the conventional gradient-enhanced

model to the localizing approach yields a more realistic damage pattern in the 1D tensile test. However, the predictions in the structural simulations of the L-shaped specimen test are not satisfactory. In particular, the ultimate load is overestimated significantly.

Future research efforts should focus on a more comprehensive investigation of the localizing gradient-enhanced model. In particular, the impact of this straightforward extension has to be studied in a comprehensive set of numerical experiments, including a wide range of failure modes. Moreover, the formulation of the exponential softening law $\omega(\bar{\beta})$ should be revisited. A reformulation may improve the predictions of the localizing approach in structural simulations. Furthermore, the influence of the formulation of the scaling function $g(\omega)$ on the results should be studied in more detail. A more refined relation may be needed to obtain better results in structural simulations.

References

[1] Z. P. Bažant and M. Jirásek. "Nonlocal integral formulations of plasticity and damage: survey of progress". In: *J. Eng. Mech.* 128.11 (2002). Publisher: American Society of Civil Engineers, pp. 1119–1149.

[2] A. Dummer, M. Neuner, and G. Hofstetter. "An extended gradient-enhanced damage-plasticity model for concrete considering nonlinear creep and failure due to creep". In: *Int. J. Solids Struct.* 243 (2022), p. 111541.

[3] P. Grassl and M. Jirásek. "Damage-plastic model for concrete failure". In: *Int. J. Solids Struct.* 43.22-23 (2006), pp. 7166–7196.

[4] P. Grassl and M. Jirásek. "Plastic model with non-local damage applied to concrete". In: *Int. J. for Numer. Anal. Methods Géoméch.* 30.1 (2006), pp. 71–90.

[5] C. Miehe, F. Welschinger, and M. Hofacker. "Thermodynamically consistent phase-field models of fracture: Variational principles and multi-field FE implementations". In: *Int. J. for Numer. Methods Eng.* 83.10 (2010), pp. 1273–1311.

[6] M. Neuner, P. Gamnitzer, and G. Hofstetter. "A 3D gradient-enhanced micropolar damage-plasticity approach for modeling quasi-brittle failure of cohesive-frictional materials". In: *Comput. & Struct.* 239 (2020), p. 106332.

[7] M. Neuner et al. "From experimental modeling of shotcrete to numerical simulations of tunneling". In: *Advances in Applied Mechanics*. Vol. 54. Elsevier, 2021, pp. 205–284.

[8] R. H. J. Peerlings, R. De Borst, W. A. M. Brekelmans, and J. H. P. De Vree. "Gradient enhanced damage for quasi-brittle materials". In: *Int. J. for Numer. Methods Eng.* 39.19 (1996), pp. 3391–3403.

[9] L. Poh and G. Sun. "Localizing gradient damage model with decreasing interactions". In: *Int. J. for Numer. Methods Eng.* 110.6 (2017). Publisher: Wiley Online Library, pp. 503–522.

[10] K. Willam and E. Warnke. "Constitutive model for the triaxial behaviour of concrete". In: *Seminar on Concrete Structures Subjected to Triaxial Stresses*. Vol. 19. Bergamo, Italy, 1975, pp. 1–30.

[11] B. Winkler, G. Hofstetter, and H. Lehar. "Application of a constitutive model for concrete to the analysis of a precast segmental tunnel lining". In: *Int. J. for Numer. Anal. Methods Géoméch.* 28.7-8 (2004). Publisher: Wiley Online Library, pp. 797–819.

[12] D. Zhao, B. Yin, S. Tarachandani, and M. Kaliske. "A modified cap plasticity description coupled with a localizing gradient-enhanced approach for concrete failure modeling". In: *Comput. Mech.* 72.4 (2023), pp. 787–801.

[13] I. Zreid and M. Kaliske. "A gradient enhanced plasticity–damage microplane model for concrete". In: *Comput. Mech* 62.5 (2018). Publisher: Springer, pp. 1239–1257.